Current and Plasma Oscillation Inspection in PPS®-X000 HET Thruster – EMD Approach

IEPC-2007-239

Presented at the 30th International Electric Propulsion Conference, Florence, Italy
September 17-20, 2007

Jacek Kurzyna[*] Karol Makowski[†] and Zbigniew Peradzyński[‡]
Institute of Fundamental Technological Research, Polish Academy of Sciences,
Świętokrzyska 21, 00049 Warsaw, Poland

and

Alexey Lazurenko[§] Stephane Mazouffre[¶] Giovanni Coduti [‖] and Michel Dudeck[**]
ICARE – CNRS, 1C Avenue de la Recherche Scientifique, 45071 Orléans Cedex 2, France

Local plasma oscillations in correlation with discharge current and cathode potential variation are studied in a high voltage (HV) Hall effect thruster (HET) PPS®-X000. A set of electric probes is used to pick-up the signals. The probes are located in the thruster channel exit zone beyond its outer circumference. In a number of runs the probe locations and external potential as well the thruster operating conditions (voltage in the range of 200-900 V and xenon flow rate) were varied. Captured non-stationary signals are expanded into finite sets of intrinsic modes with the use of Empirical Mode Decomposition (EMD) method. Hilbert-Huang power spectra indicate characteristic bands in LF (tens of kHz), MF and HF (tens of MHz) range. However, HF emission as regular as had been observed in our previous studies of low voltage PPS-100 thruster now is observed only in some particular operating conditions. When the supplying voltage is low (e.g. 400 V) the known electrostatic drift wave propagating along the thruster azimuth is unambiguously identified in the probe signals. For higher voltages HF spectra are usually broadband and do not indicate characteristic, well defined pikes. HF emission becomes very irregular or even seems to be random. On the other hand, when regular wave appears (intermittently or in sequences of bursts) the frequencies from the band of $\approx 5 \div 100$ MHz are resolved. In contrary, the oscillations of MF band that previously had been resolved with some uncertainty now appear to dominate in discharge current when the thruster is supplied with the highest voltages. Intense oscillations of MF range are identified with the use of positively polarized probes and examining variations of cathode potential and discharge current. The correlations of all mentioned signals are evident in this frequency band. Correlating oscillations of HF band with MF wave of discharge current one can deduce that triggering of HF oscillations for the highest voltages now is controlled by appropriate phase of MF wave while at lower voltages (and for PPS-100 thruster) is controlled by the phase of breathing mode (LF band).

[*]Dr., jkurzyna@ippt.gov.pl.
[†]Dr., kmak@ippt.gov.pl.
[‡]Prof., Department of Mathematics, Computer Sciences and Mechanics, Warsaw University, 02097 Warsaw, Poland, zperadz@mimuw.edu.pl
[§]Dr., lazurenk@cnrs-orleans.fr.
[¶]Dr. mazouffre@cnrs-orleans.fr.
[‖]Dr. Giovanni.Coduti@cnrs-orleans.fr.
[**]Prof. dudeck@cnrs-orleans.fr.

I. Introduction

Being currently under examination at *ICARE–CNRS* Hall effect thruster PPS®-X000 is a high voltage successor of PPS-100 one. With discharge voltage up to 1 kV and power of $\sim$6 kW it results in maximal thrust of $\sim$330 mN and specific impulse of $\sim$3200 s (Ref. 1). Thus producing thrust four times higher than that of PPS-100, while xenon flow rate does not exceed two times the previous one, it is a promissing engine in terms of plasma propulsion for space missions.

Studies of operational envelope of the thruster have to be accompanied with examination of its discharge and plasma stability. Therefore in our experiment discharge current as well local plasma oscillations were examined. The discharge current was regarded to be the main reference characteristics. It was measured directly in the electric circuit of the thruster. In addition, time variations of thruster cathode potential against the ground were measured in a number of runs. The related local plasma oscillations were captured with the set of unbiased electric probes operating close to the ground potential or biased with both positive and negative voltages. The time series that represent plasma oscillations were recorded for discharge voltage varied in the range of 200$\div$900 V while xenon mas flow rate was varied from 5 to 9 mg/s. In these series of measurements magnetic field was kept constatnt.

Even visual inspection of signals collected during operation of Hall effect thruster (HET) indicates that they are nonstationary in the time scale of the measurements and often of intermittent nature. Thus for analysis of these signals we have used a relatively new method suggested by N. Huang (Ref. 2) and called *Empirical Mode Decomposition* (EMD). Therefore we summarize this method in the next section. In the subsequent section the brief description of the experiment is presented. Finally, the obtained results are discussed and conclusion is drawn.

II. Empirical Mode Decomposition

When nonstationary signals are to be analyzed the well known Fourier methods are not a proper tool. The reason is that the "frequency content" of any interval of not periodic signal varies in time. In such a case insteed of Fourier power spectra *instantaneous frequency* and *power* corresponding to it are often examined, like for frequency modulated signals. Instantaneous frequency is usually defined as a time derivative of the phase of a complex function $z(t)$ that is to be built using given real signal $s(t)$ and an orthogonal to it function $\tilde{s}(t)$ (see e.g. Ref. 3).

Thus, one can ask about the intensity and rate of variations of the analyzed signal at any moment in time. However, searching for function $\tilde{s}(t)$ orthogonal to given $s(t)$ is not a unique routine. According to Gabor[4] definition of the needed complex function $z(t)$ the identity of its Fourier transform and Fourier transform of a given signal $s(t)$ is required for positive frequencies. For negative frequencies Fourier transform of $z(t)$ have to vanish. It is easy to show[4,5] that when imaginary part of the complex function $z(t)$ is defined by Hilbert transform of its real part the both conditions are fulfilled. Therefore, for a given real signal $s(t)$ the following definition of required complex signal is applied: $z(t) = \mathcal{A}[s(t)] \stackrel{\text{def}}{=} s(t) + i\mathcal{H}[s](t)$ where:

$$\mathcal{H}[s](t) \stackrel{\text{def}}{=} \frac{1}{\pi}\,\mathrm{Pv}\int_{-\infty}^{\infty}\frac{s(\tau)}{t-\tau}d\tau \stackrel{\text{ozn}}{=} \tilde{s}(t)\,, \tag{1}$$

is the Hilbert transform of $s(t)$, and Pv principal value of the integral. $\mathcal{A}[s(t)]$ is called an *analytical signal*. Thus one can write at once: $z(t) = A(t)\exp(i\varphi(t))$, and instantaneous frequency of the calculated analytical signal is defined as a derivative of our complex function argument $\varphi(t)$: $\omega_I(t) \stackrel{\text{def}}{=} d\varphi(t)/dt$ and instantaneous power as a square of its amplitude $A(t)$, where as usual: $A(t) \stackrel{\text{def}}{=} \sqrt{s^2(t) + \tilde{s}^2(t)}$ is a module of a complex function.

However, for general class of signals $s(t)$ the instantaneous frequency may lose physical meaning because its value can become negative. Such signals are often called multi-component. Representation of a given multi-component signal as a sum of k simpler components $s_k(t)$ (*mono-component signals*) with well behaved instantaneous frequency ω_k (t) is the solution. Thus, one can write:

$$s(t) = \sum_{k=1}^{N} s_k(t) = \Re[\sum_{k=1}^{N} a_k(t)exp(i\varphi_k(t))] = \Re[A(t)\exp(i\varphi(t))]\,, \tag{2}$$

where each elementary analytical signal $\mathcal{A}_k[s_k(t)] = s_k(t) + i\mathcal{H}[s_k](t) = z_k(t)$ is determined by $s_k(t)$ and its Hilbert transform. For each term of the sum one can find its amplitude $a_k(t)$ and instantaneous frequency $\omega_k(t) = \dot{\varphi}_k(t)$.

In complex plane mono-component signals are represented by trajectories $z_k(t)$ rotating around a fixed center. Such trajectories are called *proper rotations*.[6] In contrary, the complex trajectory of a multi-component signal exhibits a number of loops with moving instantaneous centers of rotation. That is why the arguments of such trajectories are not monotonic functions of time and instantaneous frequency has not clear physical meaning.

Having multi-component signal expanded into a set of mono-componet terms power carried by each term is a function of time and instantaneous frequency. Hence, the resulting power spectrum of a nonstationary signal may be composed by several components (modes) that depend on two variables: time and instantaneous frequency. Defined by the algorithm Empirical Mode Decomposition (EMD) method is known as a self-adaptive routine that can expand the general class of signals into a sum of simpler components – *intrinsic mode functions – imf*s.[2] Each such component is a desired monocomponent signal. Often some of intrinsic modes have a clear interpretation and represent physical modes that are present in the studied process. That is why EMD method is so attractive despite it has not got a mathematical background yet. Power spectrum built up of instantaneous frequencies that are calculated for a set of intrinsic mode functions is called *Hilbert-Huang spectrum*. To summarize:

- Given nonstationary signal is decomposed into a set of monocomponent intrinsic modes with the use of self-adaptive method called EMD
- Application of the Hilbert transform to the whole set of modes allows to identify peculiar events and assign them a range of instantaneous frequency and power.

For the detailed description of the method the reader is referred to Huang's et al. original paper (Ref. 2) and the review paper (Ref. 7). Here, we only summarize the method to remind the main steps of it. Let us start with the definition of intrinsic mode functions that are generated with EMD method.

Definition 1 *To be an* ***intrinsic mode function*** $imf(t)$*, it must fulfill two conditions:*

1. *the number of its zero crossings and extrema may differ at most by one;*
2. $imf(t)$ *has to be symmetric with respect to its local mean value which must tend to zero at any point.*

The estimation of a *local mean value* $m(t)$ of a given $s(t)$ is crucial to the EMD method. Usually it is done calculating the average value of *upper* $\mathrm{upp}(t)$ and *lower* $\mathrm{low}(t)$ *envelopes* of $s(t)$. The appropriate envelopes are interpolated using natural cubic splines with nodes in maxima (for $\mathrm{upp}(t)$) or minima (for $\mathrm{low}(t)$) of $s(t)$. However, there are other possibilities, for instance $m(t)$ can be estimated by B-spline curve determined on the all local maxima and minima of $s(t)$ simultaneously.[8] In such a case one avoids searching for the envelopes. The authors have tested this approach and found it similarly usefull as the original method of Huang (Ref. 2). Thus, the EMD algorithm can be summarized as follows:

- starting with subtraction of the local mean $m(t)$ from the signal $s(t)$ results in the first *candidate* to be an *intrinsic mode function*
- if the conditions of definition 1 are not satisfied the subtraction of a local mean is now applied to **the first candidate** resulting in the second candidate *etc.* Finally, if the conditions are fulfilled the last candidate is regarded as an intrinsic mode (this iterative routine is called *sifting procedure*)
- the obtained intrinsic mode is now subtracted from the signals resulting in its residue (or from the previous residue for subsequent modes)
- the *residue* is proceeded in the same way resulting in the second intrinsic mode,
- and so on ...
- up to the last residue which cannot be farther decomposed due to the lack of more than two extrema
- finally Hilbert transform is applied to the whole set of intrinsic modes resulting in *time–instantaneous frequency–power* distribution and thus desired Hilbert-Huang spectrum.

EMD method had been successfully applied to study Hall Effect Thruster (HET) plasma oscillations as measured by means of array of antennas and electric probes galvanically coupled to plasma.[9–13] In those papers one can find more details of the procedure that had been applied for calculation of analytical signals, searching for instantaneous frequencies, construction of Hilbert-Huang and marginal power spectra as well looking for the phase lock and some remarks on error sources. The current studies are continuation of the previous ones and we present here results for the new, high voltage thruster PPS®-X000.

III. Experiment

Hall effect thruster PPS®-X000 has been operated at the PIVOINE ground-test facility[14] located at ICARE-CNRS. The new thruster is designed to be supplied with voltage even two times higher than the previous model PPS-100. Thus, a number of runs were done to study new thruster properties (stability of the discharge current, efficiency *etc.*) at different operating conditions – discharge voltage was varied in the range of $200 \div 900$ V and xenon flow rate in the range of $5 \div 9$ mg/s. Here, we are mainly interested in local oscillations (or instabilities) of plasma in the thruster exit zone referred to global oscillations of discharge current and cathode potential variations.

Discharge current oscillations were directly monitored at the thruster power circuit by means of Tektronix current probe connected to Tektronix TDS5104 oscilloscope. Usually the discharge current I_A was measured at the thruster anode side. Additionally, in some experiments, the total current I_C was recorded at the cathode side. The cathode potential, when registered was measured against the ground level.

Local MF and HF oscillations were captured with the use of electric probes installed at the outer circumference of the thruster, close to the maximum of magnetic barrier.[15] Classical Langmuir probes, in galvanic contact with plasma were applied. The signalas were recorded when the oscilloscope was operated in AC mode at sampling frequency of 1.25 GHz. All the transmission lines were of equal length and terminated according to their 50 Ω impedance. In separate runs polarizing voltage of the probes was varied in the range of $-30 \div +50$ V (in 10 V steps). However, the probes were mostly not polarized and in such a way operated close to the ground potential.

The location of the probes is shown in Figure 1 a and 1 b. Four millimeter long probe tips with diameter of 0.2 mm were oriented radially. P_1 and P_2 probes composed a stiff tandem with tip separation of 10 mm or 11 mm. When the tandem was oriented in (r, z) plane the signals of P_3 probe was additionally recorded. The angle between P_3 probe and (r, z) plane of the tandem was constant and equal to $\pi/2$ – see Figure 1 b.

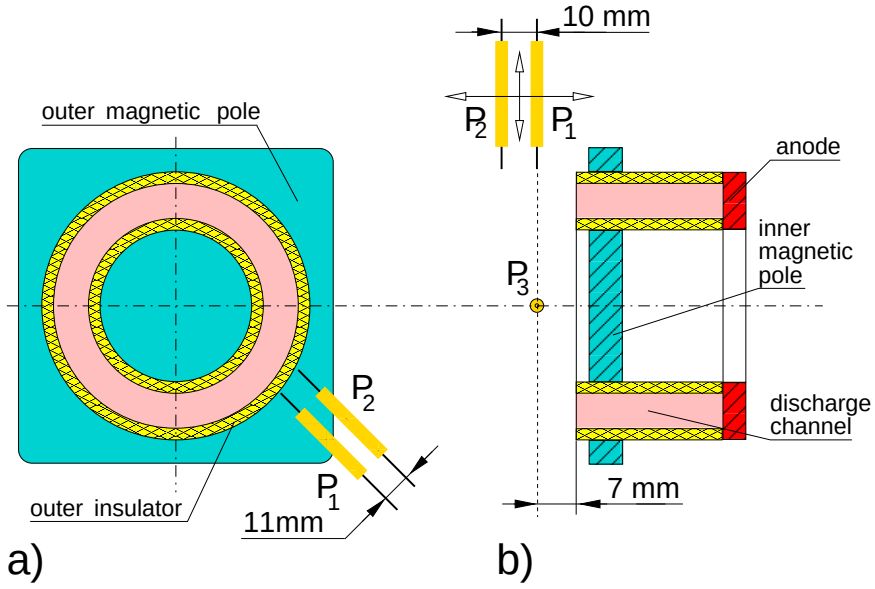

Figure 1. Electric probes used in the experiment: *a*) **P_1 and P_2 probe tandem in a fixed location at (r, ϑ)plane,** *b*) **P_1 and P_2 probe tandem in a fixed azimuthal location at (r, z) plane – shown is P_3 probe with azimuth of $\pi/2$ against P_1–P_2 tips plane**

The propagation of HF waves along the discharge channel circumference was studied when two of the probes were located in different azimuthal positions but in the same (r, ϑ) plane. When the tandem was positioned in (r, z) plane of the thruster 10 mm separation between probe tips allowed us to follow the longitudinal propagation. In a number of runs r and z coordinates of $P_1 - P_2$ tandem were changed. However, to protect the probe tips against direct exposition to the stream of plasma, they were always kept in the shade of the outer insulator.

IV. Results and discussion

Nonstationary signals representing discharge current, variation of cathode potential and electric probe currents were studied using their raw records as well they were expanded into finite sets of intrinsic mode functions *imf*'s with the use EMD method.[2] The analysis is applied to the signals captured in different operating conditions – as it was mentioned above discharge voltage was varied in the range of $200 \div 900$ V and xenon flow rate of $5 \div 9$ mg/s.

A. Lower voltage range: $U_D \leq 550$ V

1. P_1 and P_2 probes in (r, ϑ) plane, 6 mg/s xenon flow rate

Comparing waveforms of U_C and discharge current as measured in the thruster circuit it is obvious that time intervals between cathode potential extrema are two times shorter than appropriate intervals of the *breathing mode* visible in I_C or I_A signals. Typical waveforms of the corresponding raw signals are presented in Figure 2 a and 2 b for discharge voltage $U_D = 350$ V and $U_D = 550$ V respectively. Even with visual

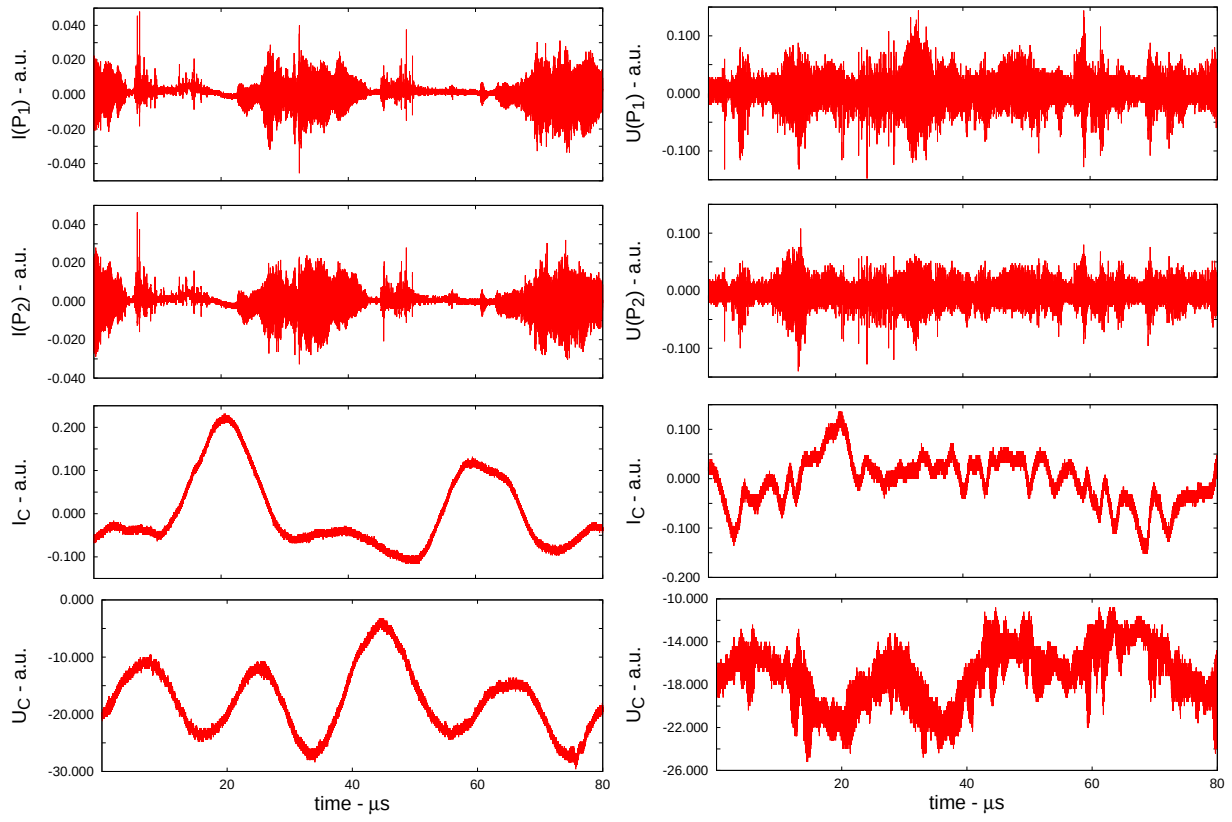

(a) (b)

Figure 2. Raw signals $I(\mathrm{P}_1)$, $I(\mathrm{P}_2)$, I_C and U_C as captured for xenon flow rate of 6 mg/s when P_1 and P_2 probes were positioned in (r, ϑ) plane; *a*) $U_D = 350$ V, *b*) $U_D = 550$ V.

inspection of the waveform of I_C corresponding to $U_D = 550\,\mathrm{V}$ one can resolve significant oscillations of MF range at the background of the breathing mode. They are also well resolved in the raw U_C signal despite that the noise level in this signal is much higher than in I_C. The corresponding intrinsic modes are ambiguously extracted with EMD method. The instantaneous frequency band of considered here MF oscillations ($\sim 200\,\mathrm{kHz}$ and higher) corresponds to characteristic frequency of transit time oscillations[16,17] that are expected in the studied thruster.

P_1 and P_2 probes were not polarized in this series of measurements. Therefore the both were operated close to the ground potential (perhaps in the vicinity of the low knee of $I-V$ probe characteristics which will be discussed later) and MF wave could not be reliably resolved even with so sensitive method as EMD in its classic version. However, HF emission was perfectly recorded.

For $U_D = 350\,\mathrm{V}$ one can notice the satisfactory reproducibility of I_C and U_C records.

2. *P_1 and P_2 probes in (r,ϑ) plane, 7.3 mg/s xenon flow rate, $U_D = 350$ V*

In this series of measurements discharge current as captured at the anode side and cathode potential were used as the reference global characteristics. P_2 probe was not polarized as in the previous case. However, the voltage applied to P_1 probe was varied in the range $0 \div +50\,\mathrm{V}$ in steps of $10\,\mathrm{V}$. Also, some number of runs had been recorded for P_1 probe polarized with $-20\,\mathrm{V}$. As an example raw signals representing I_A, U_C and currents of positively biased P_1 probe as well unbiased P_2 probe are reproduced in Figure 3 a. Most significant modes extracted with EMD method and corresponding Hilbert-Huang spectrum in MF range is also depicted in the right panels of the same figure. The average frequency of the fastest intrinsic mode

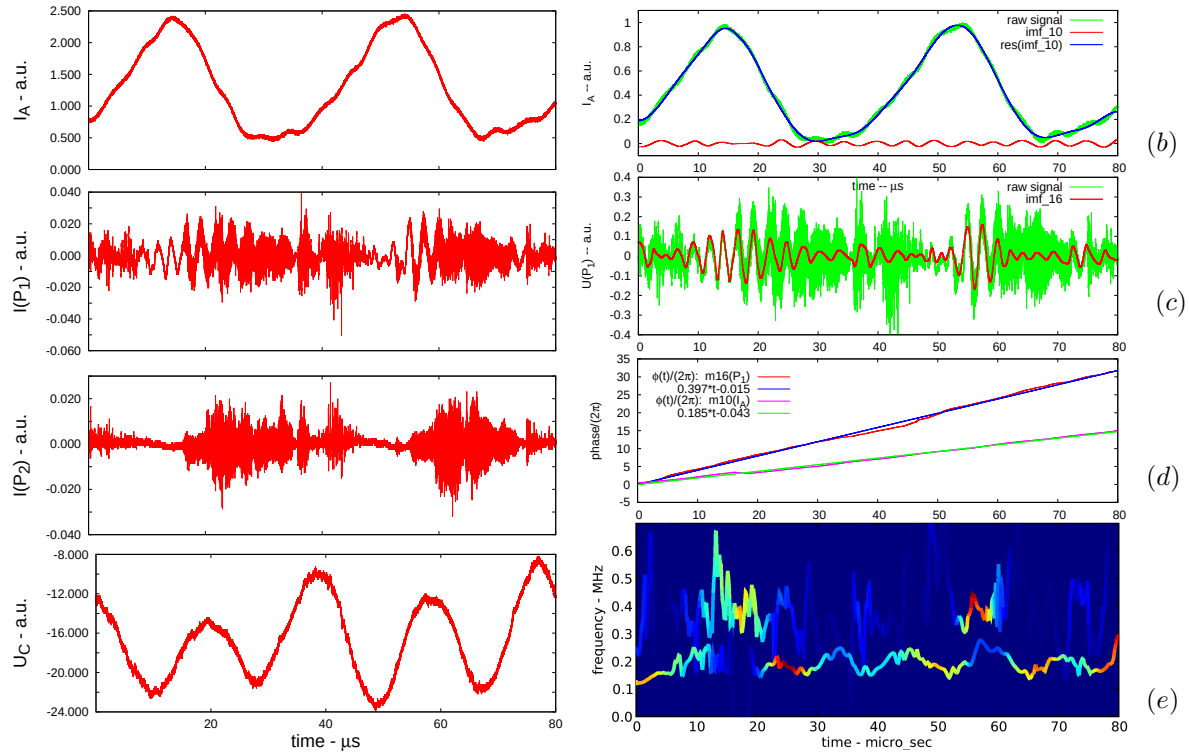

Figure 3. P_1 and P_2 probes in (r,ϑ) plane, 7.3 mg/s xenon flow rate, $U_D = 350\,\mathrm{V}$; *a*) discharge current I_A, $I(P_1)$, $I(P_2)$ and U_C with respect to the ground – raw signals. *b*) Normalized discharge current I_A (in green), its intrinsic mode imf_{10} (in red) and the residue $res(imf_{10})$ (in blue) that corresponds to *breathing mode*. *c*) normalized $I(P_1)$ signal (in green) and its intrinsic mode imf_{16} (in red) that corresponds to the average frequency of ≈0.4 MHz – probe biased with $+40\,\mathrm{V}$. *d*) Phase $\varphi(t)$ calculated for intrinsic mode $imf_{10}(I_A)$ of discharge current I_A and $imf_{16}(P_1)$ of P_1 probe signal. The inclination of the best fitted straight lines corresponds respectively to ≈0.2 and ≈0.4 MHz. *e*) Hilbert spectra of the appropriate intrinsic modes for P_1 probe (upper curve) and discharge current I_A (lower curve) – MF range.

HF emission starts with average frequency of about $40 \div 50\,\mathrm{MHz}$. After $2 \div 4$ microseconds the waveform of HF emission turns into more regular sequence of very sharp pikes of variable amplitude. The almost constant intervals between the pikes as well the cross correlations between P_1 and P_3 probe signals allow us to calculate the basic period of HF emission cycle. For the case that is discussed here this period varies from $\approx 6.4\,\mathrm{MHz}$ to $\approx 6.7\,\mathrm{MHz}$ in correspondence to the chosen maximum of discharge current I_A. The measured time delay Δt between signals of P_1 and P_3 probes is equal to $\approx 41\,\mathrm{ns}$. This value gives us circular frequency $\omega = 2\pi\nu \approx 2\pi \cdot 6.1 \times 10^6\,\mathrm{rad/s}$. On the other hand for channel outer diameter of $0.15\,\mathrm{m}$ the measured Δt gives us the velocity of azimuthal propagation $v_\vartheta \approx 2.9 \times 10^6\,\mathrm{m/s}$. Assuming that this value corresponds to the speed of electron drift along the azimuth in radial magnetic field $B_r = 15\,\mathrm{mT}$ one calculates the value of axial electric field $E_z = v_\varphi B_r \approx 4.3 \times 10^4\,\mathrm{V/m}$. This vale is about 1.5 times of that reported for PPS-100 thruster. Similar value of $E_z = v_\vartheta B_r \approx 4.45 \times 10^4\,\mathrm{V/m}$ was calculated basing on the signal of an additional P_4 probe was considered. When used P_4 probe was positioned at the azimuth of π with respect to P_1 probe.

Usually, in operational conditions of the thruster corresponding to lower voltages (*e.g.* $U_D = 350\,\mathrm{V}$ and xenon flow rate of 5, 6 or $7.3\,\mathrm{mg/s}$) HF emission is correlated with each decreasing phase of the *breathing mode* that governs the discharge current. The same behavior had been observed for PPS-100 HET. In contrary, for $U_D = 550\,\mathrm{V}$, when additional MF oscillations appear in global signals HF emission is observed almost permanently. It is worth to note that its intensity varies irregularly or even abruptly. For both U_D voltages pikes of 7, 14 19, 27, 60 i $110\,\mathrm{MHz}$ are resolved in the appropriate power spectra of HF emission.

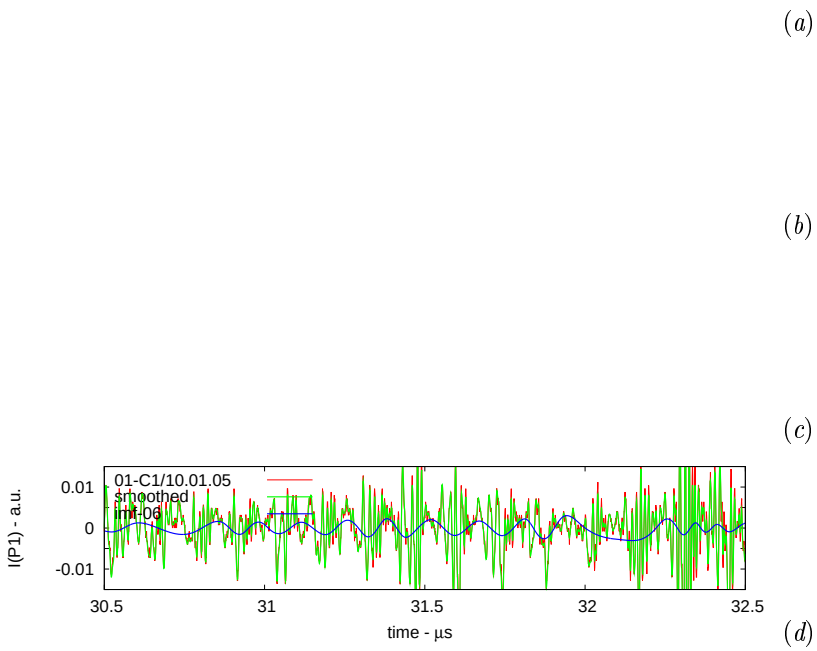

Figure 5. Expanded view of HF intrinsic modes resulting due to application of EMD to P_1 probe signal captured at $U_D = 350\,\mathrm{V}$ and xenon float rate of 7.3 mg/s – the probe was unbiased; *a*) and *b*) imf_{01} fragments, *c*) – imf_{04} fragment and *d*) – imf_{06} fragment. Raw signals are shown in red, smoothed with Gaussian filter in green, and intrinsic mode functions in blue.

Studying Hilbert-Huang power spectra of the decomposed probe signals at the voltage $U_D = 350\,\mathrm{V}$ one can notice the similar average frequencies as mentioned above. However, they corresponds to particular intrinsic modes and may be limited to short intervals that appear locally in time – see Figure 4.

HF emission when correlated with the decreasing phase of the breathing mode usually starts with regular oscillations of the order of $60\,\mathrm{MHz}$ (see Figure 5 a). This phase may last about $1\,\mu\mathrm{s}$. Next, even

faster oscillations that can be grouped into a sequence of packages may appear. The frequency within each package is modulated and reaches 100 MHz or more (Figure 5 b). The duration of distinguished packages corresponds to the period of the expected azimuthal electrostatic wave. Additionally, the intervals of more regular oscillations with frequency of about 20 MHz are resolved (Figure 5 c). The slowest intrinsic modes of HF band (here imf_{06}) may follow the waveform of envelopes that correspond to the distinguished packages (Figure 5 d).

To follow the azimuthal propagation 11 mm separation of the P_1 and P_2 probes positioned in (r, ϑ) plane seems to be too low.

B. Upper voltage range: $U_D > 500$ V

In this section we discuss the results that were obtained when xenon flow rate was reduced to 5 mg/s. Here P_1 and P_2 probes were positioned in (r, z) plane – see Figure 1 b. All three probes P_1, P_2, and P_3 were unbiased. Typical raw signals are reproduced in Figure 6 for discharge voltage $U_d = 500$, 700, and 900 V. One can notice at once that the waveform of discharge current I_A is very irregular for $U_d = 700$ V. Thus, it is obvious that for this voltage we find much worse reproducibility of discharge current in subsequent runs than one can find for both remaining voltages. However, the general conclusion can be also drawn for $U_d = 700$ V.

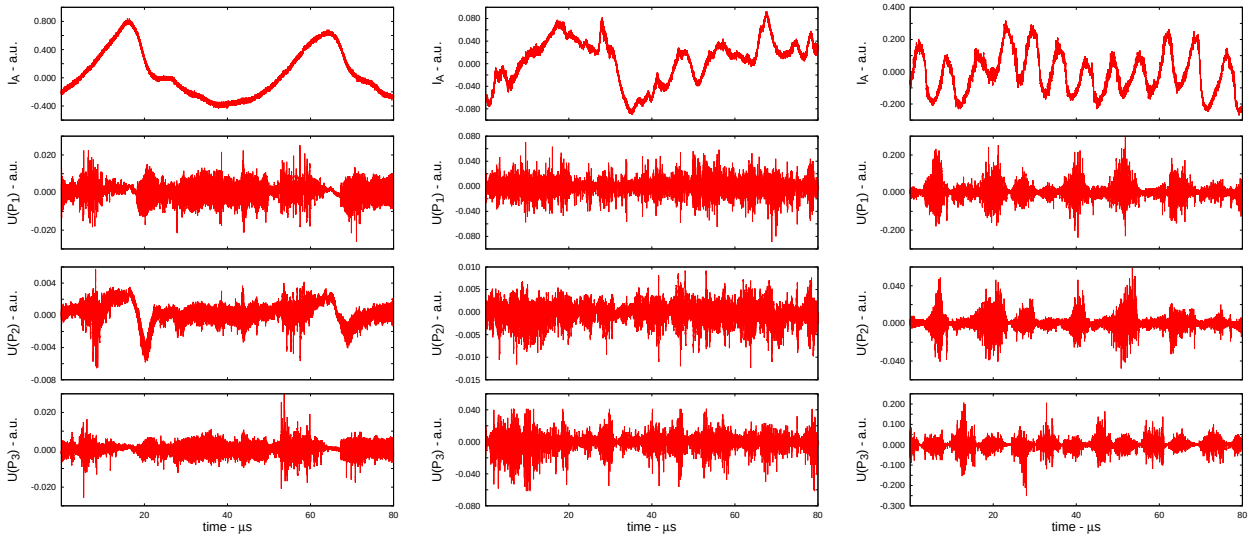

Figure 6. Raw signals corresponding to discharge current I_A and currents of P_1,P_2, and P_3 probes – 5 mg/s xenon flow rate; *a*) $U_D = 500$ V, *b*) $U_D = 700$ V, *c*) $U_D = 900$ V.

1. *MF range*

Also in this case EMD method was used to extract sets of intrinsic modes from signals representing discharge and electric probe currents. And thus, in Figure 7 we have depicted the sequences of imf's corresponding to discharge currents that are reproduced in Figure 6. With the use of EMD it is easy to resolve intrinsic modes of MF range. In the considered here operating conditions the amplitudes of these modes are comparable with the amplitude of I_A as a whole.

It is evident that well known breathing mode (with average frequency of $\sim$ 20 kHz) dominates for $U_d = 500$ V and is almost completely represented by imf_{10}. For this voltage intrinsic modes of MF range are extracted as separate oscillations or wiggles (i.e. events that may last from one to several cycles) that are correlated with decreasing phase of breathing mode cycles. Increasing U_d voltage to 700 V one can notice that intrinsic modes of MF range turn into irregular but continuous wave of the amplitude that can be comparable with the amplitude of the breathing mode – see Figure 7 b. And finally, for $U_d = 900$ V intrinsic modes of MF become more regular (here imf_{10} with average frequency of $\approx$ 150 kHz) and their amplitude may be even bigger than that of suppose to be breathing mode (represented perhaps by imf_{12}) – see Figure

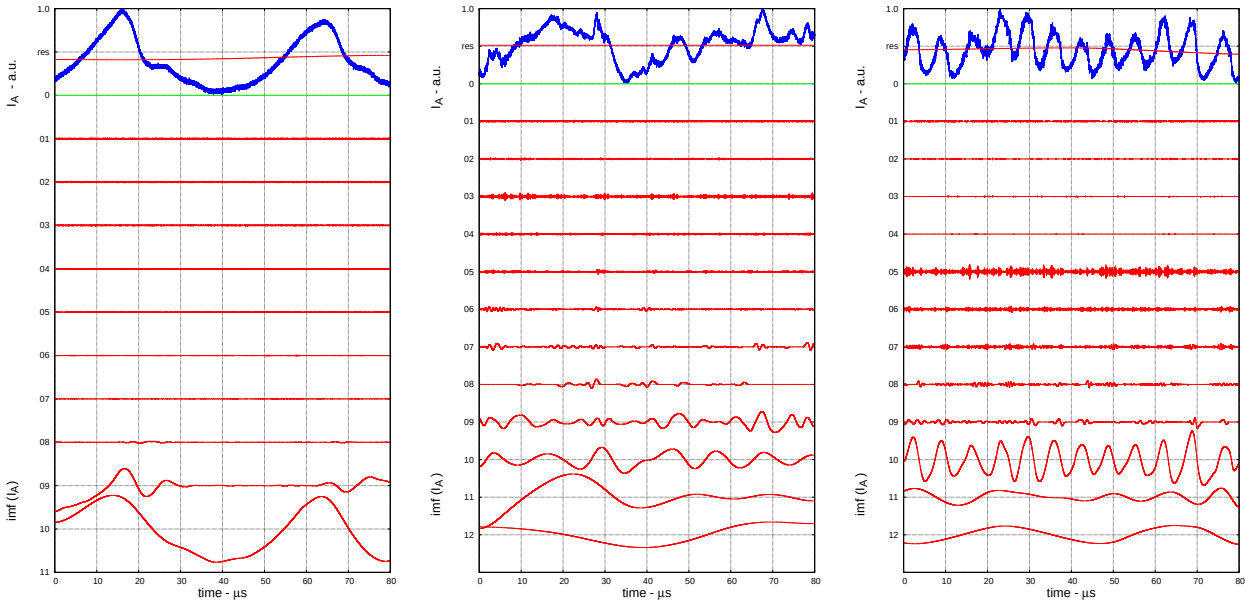

Figure 7. Empirical mode decomposition of I_A currents: *a*) discharge voltage $U_D = 500$ V, *b*) $U_D = 700$ V, and *c*) $U_D = 900$ V. Raw signals are shown in blue and resulting intrinsic modes in red. EMD method with treatment of intermittences was applied. Xenon flow rate of 5 mg/s.

7 c. It is worth to note that amplitudes of the slowest intrinsic modes that correspond perhaps to physical breathing mode (with average frequency of the order of 20 kHz) decreases with the growth of U_d. And in contrary, the amplitudes of intrinsic modes of MF range increase with the growth of U_d. Moreover the instantaneous frequency of these modes tends to stabilize at the average value of about $150 \div 200$ kHz. These facts are well documented in a number of runs.

2. HF range

As it was mentioned above HF emission is usually triggered during each decreasing phase of any I_A cycle and ceases before discharge current reaches its subsequent maximum. This view is evident for discharge voltage $U_D = 500$ V and was previously reported for PPS-100 thruster (Ref. 12, 18). Also for $U_D = 900$ V similar correlation can be confirmed. However, for this high voltage the basic frequency of discharge current I_A is much higher (~ 150 kHz) than it was for $U_D = 500$ V. Moreover, the amplitude of I_A varies irregularly in time. It may be the reason that HF emission bursts have not enough time to rise up to similar level in subsequent cycles of I_A. For discharge voltage $U_D = 700$ V HF emission is very irregular, lasts almost permanently and we cannot reliably detect when it starts or ceases.

On the other hand in bursts of HF emission captured with P_1, P_2, and P_3 probes we can resolve some intervals of more regular oscillations (farther called as *packages*) with average frequencies in the range of $50 \div 100$ MHz (the appropriate fragment of imf_{04} that was extracted from P_3 probe signal is depicted in Figure 8 c. Usually these packages have the length of several cycles and appear in sequences. Time intervals between subsequent packages correspond to average repetition frequency of about $4 \div 5$ MHz. It is worth to note that each observed sequence of packages is correlated with deep modulation of discharge current I_A – e.g. for $U_d = 900$ V corresponding to MF modes of 150 kHz. One can ask if due to fast and deep modulation of I_A the expected azimuthal electrostatic wave has not got enough time for its full development.

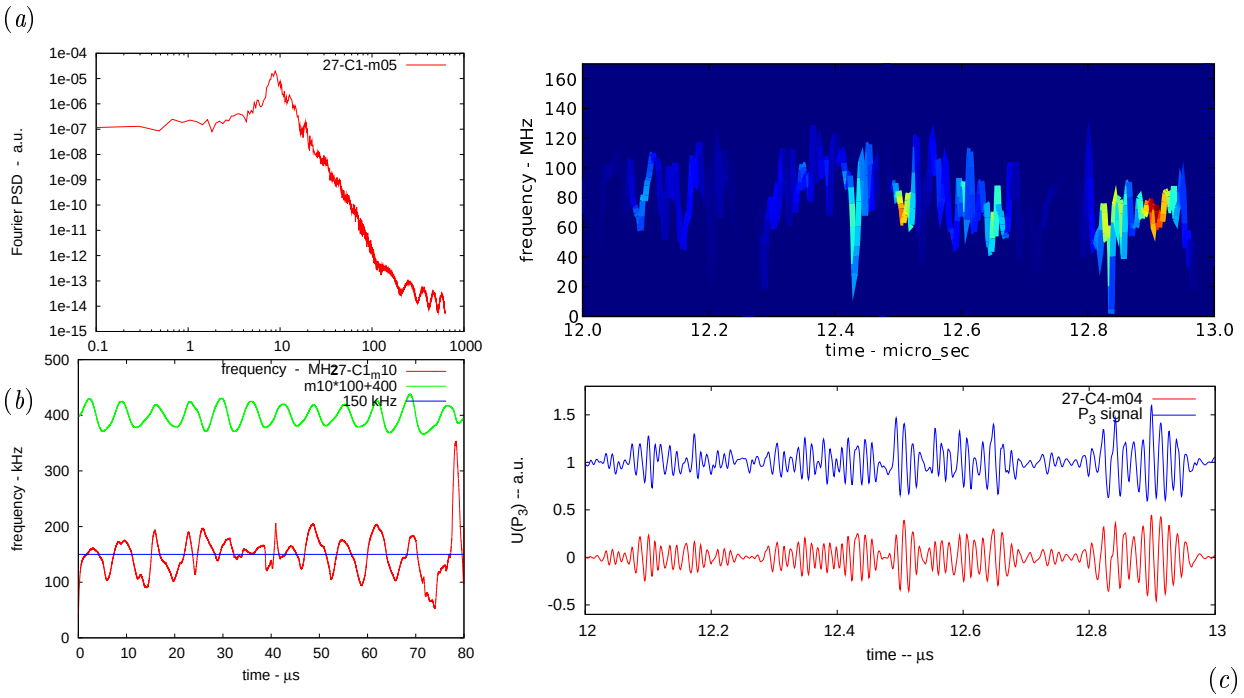

Figure 8. Spectral characteristics of the chosen intrinsic modes resulting for thruster operated at $U_d = 900$ V and xenon flow rate of 5 mg/s: *a*) Fourier PSD of imf_{05} resulting with EMD applied to I_A, *b*) instantaneous frequency $\nu(t)$ of imf_{10} from the same set intrinsic modes (red curve) – additionally rescaled mode imf_{10} is shown in green, *c*) in upper panel Hilbert-Huang spectrum of imf_{04} fragment from decomposition of P_3 probe signal; in lower panel the corresponding fragments of this mode (in red) and raw P_3 probe signal (in blue).

V. Conclusion

New model of high voltage Hall effect thruster is studied in the wide range of operating conditions. The oscillations of global thruster characteristics like discharge current and cathode potential variation are measured directly in the electric circuit of the thruster. The local fluctuations of plasma are captured with electric probes positioned in the exit zone of the thruster. Empirical mode decomposition method for analysis of recorded nonstationary signals is applied. Characteristic bands of instantaneous frequency are identified by means of Hilbert-Huang transform (HHT) and for some quasisteady modes with the use of traditional Fourier methods.

Studying discharge current (and variation of cathode potential) in different operating conditions a number of irregular oscillations accompanying the well known breathing mode is observed. The instantaneous frequency of these oscillations varies close to the average value of about 200 kHz. Their magnitude increases with the discharge voltage and close to 900 V can be big enough to mask breathing mode of the main discharge current. For this high voltage operational conditions the deep and fast (of about 150 kHz) current oscillations become more stable than at the lower voltages. In contrary, at lowest discharge voltages or for reduced xenon flow rate discharge current I_A seems to be clean breathing mode only.

Analyzing signals as captured with electric probes one can conclude that such regular HF emission as had been observed in PPS-100 thruster, here is found only in specific operational conditions. In such conditions the view basing on electrostatic wave that propagates along the azimuth with electron drift velocity is likely to be kept. Generally, HF emission is broadband ($\sim 5 \div 200$ MHz) and becomes very irregular or even seems to be random at higher discharge voltages. Are we dealing with the transition to turbulence in the case of irregular HF emission or could it be interpreted as an interference of several modes that circulate along the azimuth it is still an open question.

It is worth to note that at the highest voltage (900 V) HF emission appears to be correlated with deep modulation of the discharge current, now corresponding to ~ 150 kHz. One can wonder if this deep modulation of the main discharge current represents transit time oscillations that mask the known *breathing mode*, or if it is still a *breathing mode* after its possible bifurcation from a limit cycle to the invariant torus. We expect that the first hypothesis is true.

Acknowledgment

This joint work between CNRS - France and IPPT-PAN - Poland was carried out in the frame of the research group CNRS/CNES/SNECMA/Universities 2759 "Propulsion Spatiale à Plasma".

References

[1]Duchemin, O., Dumazert, P., Cornu, N., Estublier, D., and Darnon, F., "Stretching the operational envelope of the PPS®-X000 Plasma Thruster", *Proceedings of the 50th AIAA JPS&E*, Joint Propulsion Conference and Exhibit, 11–14 July, 2004, Ft. Lauderdale, FL, AIAA-2004-3605.

[2]Huang, N.E., Shen, Z., Long, S.R., Wu, M.C., Shih, H.H., Zheng, Q., Yen, N.-C., Tung, C.C., and Liu H.H., "The empirical mode decomposition and the Hilbert spectrum for nonlinear and non-stationary time series analysis", *Proc. R. Soc. Lond.*, **A 454**, 1998, p. 903

[3]Boashash, B., "Estimating and interpreting the instantaneous frequency of signal: Part I and II", *Proceedings of the IEEE*, **80**, 1992, p. 520.

[4]Gabor, D., "Theory of communication", *J. IEE (London)*, Vol. **93**, Part III, No. 26. (November),1946, pp. 429-457.

[5]Cohen, L., *Time-Frequency Analysis*, PrenticeHall Signal Processing Series, Englewood Cliffs, New Jersey 07632, 1995.

[6]Yalçinkaya, T., and Lai, Y-C., "Phase characterization of chaos", *Phys. Rev. Lett.*, **79**, 1997, p. 3885.

[7]Dätig, M., and Schlurmann, T., "Performance and limitations of the Hilbert Huang transformation (HHT) with an application to irregular water waves", *Ocean Ingeneering*, **31**, 2004, p. 1783.

[8]Liu, B., Riemenschneider, S., and Xu, Y., "Gearbox fault diagnosis using empirical mode decomposition and Hilbert spectrum", *Mechanical Systems and Signal Processing*, Volume **20**, Issue 3 , April, 2006, pp. 718-734.

[9]Kurzyna, J., Mazouffre, S., Albarede, L., Makowski, K., Peradzyński, Z., Dudeck, M., and Bonhomme, G., "Empirical mode decomposition method in application to analysis of the oscillations in a stationary plasma thruster", *German-Polish Conference on Plasma Diagnostics for Fusion and Applications*, Cracow, September 8-10, 2004.

[10]Albarède, L., *Ph.D. Thesis*, University of Orléans, France, 2004.

[11]Bonhomme, G., Enjolras, C., Kurzyna, J., Mazouffre, S., Albarede, L., and Dudeck, M., "Characterization of Hall Effect Thruster Plasma Oscillations based on the Hilbert-Huang Transform", *IEPC-2005-46*, The 29th International Electric Propulsion Conference, Princeton University, October 31 – November 4, 2005.

[12]Kurzyna, J., Mazouffre, S., Lazurenko, A., Albarede, L., Bonhomme, G., Makowski, K., Dudeck, M., and Peradzyński, Z. (2005) "Spectral analysis of Hall effect thruster plasma oscillations based on the Empirical Mode Decomposition", *Physics of Plasmas*, **12**, 2005, p. 123506.

[13]Kurzyna, J., Makowski, K., Lazurenko, A., Mazouffre, S., Dudeck, M., Bonhomme, G., and Peradzyński, Z., "Search for the frequency content of Hall effect thruster HF electrostatic wave with the Hilbert-Huang method", *PLASMA-2005 International Conference on Research and Applications of Plasmas & 3rd German-Polish Conference on Plasma Diagnostics for Fusion and Applications & 5th French-Polish Seminar on Thermal Plasma in Space and Laboratory*, Opole-Turawa, Poland, September 6–9, 2005, pp. 411-414.

[14]Bouchoule, A., Cadiou, A., Héron, A., Dudeck, M., and Lyszyk,M. "An overview of the French research program on plasma thrusters for space applications", *Contrib. Plasma Phys.*, **41**, 2001, p. 573.

[15]Lazurenko, A., Albaréde, L., and Bouchoule, A., "Physical characterization of high-frequency instabilities in Hall thrusters", *Phys. Plasmas*, **13**, 2006, p. 083503

[16]Esipchuck, Y., Morozov, A., Tilinin, G., and Trofimov, A., (1974): "Plasma oscillations in closed drift accelerators with an extended acceleration zone", *Sov. Phys. Tech. Phys.*, **18**, 1974, p. 928.

[17]Barral, S., Makowski, K., Peradzyński, Z., and Dudeck, M., "Transit time instability in Hall thruster", *Phys. Plasmas*, **12**, 2005, p. 073504.

[18]Lazurenko, A., Vial, V., Prioul, M., and Bouchoule, A., "Experimental investigation of high-frequency drifting perturbations in Hall thrusters", *Phys. Plasmas*, **12**, 2005, p. 013501.